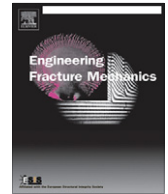




ELSEVIER

Contents lists available at ScienceDirect

Engineering Fracture Mechanics

journal homepage: www.elsevier.com/locate/engfracmech

Effect of adhesive thickness on fatigue and fracture of toughened epoxy joints – Part I: Experiments

S. Azari^a, M. Papini^b, J.K. Spelt^{a,*}^a Department of Mechanical and Industrial Engineering, University of Toronto, 5 King's College Road, Toronto, Ontario, Canada M5S 3G8^b Department of Mechanical and Industrial Engineering, Ryerson University, 350 Victoria Street, Toronto, Ontario, Canada M5B 2K3

ARTICLE INFO

Article history:

Received 14 January 2010

Received in revised form 9 June 2010

Accepted 28 June 2010

Available online 24 July 2010

Keywords:

Adhesive thickness

Fatigue crack growth

Fatigue threshold

Quasi-static fracture

Toughened epoxy

ABSTRACT

The effect of bondline thickness, from 130 μm to 790 μm , on the fatigue and quasi-static fracture behavior of aluminum joints bonded using a toughened epoxy adhesive was studied experimentally under mode-I (DCB) and mixed-mode (ADCDB) loading. Under mode-I loading, it was found that the fatigue threshold energy release rate, G_{th} , decreased for very thin bondlines, while under mixed-mode loading, the G_{th} changed very little with bondline thickness. In both cases, the effect of bondline thickness was more pronounced at higher crack growth rates. For quasi-static fracture, the effect of adhesive thickness on the energy release rate for the onset of fracture from the fatigue threshold, G_{co} , was similar to that found for the fatigue threshold; however, the steady-state energy release rate, G_c^s , increased linearly with increasing bondline thickness.

© 2010 Elsevier Ltd. All rights reserved.

1. Introduction

An understanding of the effect of bondline thickness on the quasi-static and cyclic loading behavior of adhesive joints can guide the selection of an optimal adhesive thickness and indicate the sensitivity to variations in thickness that may be caused by processing limitations.

Most studies of the effect of adhesive bondline thickness have examined quasi-static fracture under either mode-I, using DCB [1–4], tapered DCB [5–7] or compact tension [8] joints, or mixed-mode loading using cracked lap shear [9], single lap shear [10,11], modified compact tension shear [12], peel tests [13,14] or L-section joints [15]. Some investigators have observed a significant strength improvement in adhesive joints with increasing adhesive thickness [2,8,13], while others have reported no significant effect [5,9], or even a decrease [3,10,11] in strength. It has also been reported that the G_c^s , the quasi-static steady-state critical strain energy release rate, initially increases with bondline thickness and then decreases, eventually reaching a constant value [4–6,14].

Fatigue crack growth rates were found to decrease with increasing adhesive thickness under mode-I loading [1,16,17]. However, Mall and Ramamurthy [1] found that the fatigue crack growth rates in mode-I tests did not change when the bondline thickness was increased from 0.102 mm to 0.254 mm, and improved at 0.508 mm only at higher crack growth rates. At lower crack growth rates, the fatigue resistance was the same for all three bondline thicknesses. A more significant effect of bondline thickness was found when the adhesive was filled and toughened, compared to only a filled adhesive [17]. This was attributed to the larger plastic zone size of the tougher, more ductile adhesive. In general, the effect of bondline thickness on the fatigue and fracture behavior of adhesive joints has been attributed mainly to the relative size of the bondline thickness and the plastic zone ahead of the crack, with the plastic zone size being affected by the adherend restraint [4–6,14,17].

* Corresponding author. Tel.: +1 416 9785435; fax: +1 416 9787753.

E-mail address: spelt@mie.utoronto.ca (J.K. Spelt).

There have been relatively few papers dealing with the effect of bondline thickness under mixed-mode cyclic loading. Since most practical joints are loaded under mixed-mode conditions, this represents a significant gap in the literature. Schmueser [18] measured an increase in the cyclic debonding rate of mixed-mode steel cracked lap shear joints with increasing bondline thickness. The crack path in these joints was interfacial.

As mentioned above, there have been very few papers dealing with the effect of bondline thickness under mixed-mode cyclic loading, and very little work exists in the fatigue threshold region ($da/dN < 10^{-6}$ mm/cycle) for any mode ratio. The present paper describes experiments on the quasi-static and cyclic behavior of a highly-toughened epoxy adhesive as a function of bondline thickness under both mode-I (double cantilever beam) and mixed-mode (asymmetric double cantilever beam) loading. Experiments were performed for adhesive thicknesses from 130 μm to 790 μm , typical of automotive bonded joints. An accompanying paper examines these data in terms of the effect of bondline thickness on the stress distribution and plastic zone size using finite element modeling [19]. The focus of both papers is the influence of the applied strain energy release rate, G , on the plastic deformation of adhesive layers of various thickness and how the resulting differences in constraint affected the experimental fatigue and fracture observations.

2. Experimental approach

2.1. Specimen preparation

Aluminum double cantilever beam (DCB) and asymmetric double cantilever beam (ADCB) specimens (Fig. 1) were used for testing under mode-I ($\psi = 0^\circ$) and mixed-mode ($\psi = 18^\circ$) conditions, respectively. The phase angle is a measure of the mode ratio of loading, and is defined as $|\psi| = \arctan(\sqrt{G_{II}/G_I})$, where G_I and G_{II} are the modes-I and II components of the strain energy release rate. It is noted that the loading phase $\psi = 18^\circ$ is lower than in the majority of real industrial joints, better represented as cracked lap shear or single lap shear joints with $\psi \approx 50^\circ$. However, the purpose of using ADCB specimens in addition to the symmetric mode-I DCB configuration, was to cause cracks to grow near the interface of the more highly-strained adherend. It has been found that fatigue crack growth under mixed-mode loading, by promoting such asymmetric crack growth within the bondline, provides a more sensitive test of the effects of the adherend and the interfacial bond strength, particularly at slow crack growth rates near the threshold [20,21]. This is discussed further in Part II [19].

Aluminum specimens were fabricated from 12.7 mm \times 19.05 mm (1/2" \times 3/4") and 25.4 mm \times 19.05 mm (1" \times 3/4") AA6061-T651 flat bars. Prior to bonding, the substrates were abraded using a silicon carbide nylon mesh abrasive pad which produced an $R_a = 1.33 \mu\text{m}$ (standard deviation of 0.16 μm over four measurements on four different samples and for a scan length of 15 mm). The aluminum bars were then pretreated using the P2 etching process [22]. To remove the excessive adhesive after curing, the sides of the joints were sanded using a disc sander with water as a coolant, followed by a light sanding using a belt sander with 120 grit paper. To further improve the visibility of the crack and minimize any surface damage, the bondlines were finished by hand with 600 grit sandpaper, and a thin coating of diluted white correction fluid was applied to provide a high-contrast image. The failure surfaces of both the fatigue and fracture specimens showed typical, slightly curved crack fronts across the specimen width, indicating that the specimen preparation procedures did not introduce edge damage.

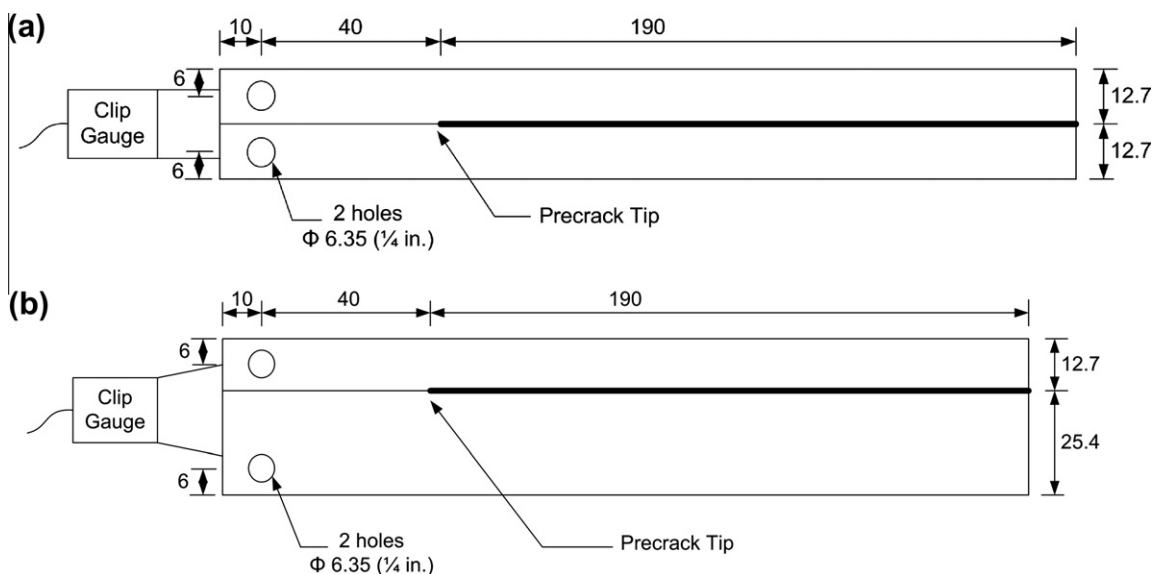


Fig. 1. Geometry of (a) DCB and (b) ADCB joints.

Specimens with three different bondline thicknesses were manufactured using spacing wires with diameters of 0.13 mm (0.005"), 0.38 mm (0.015") and 0.79 mm (0.031"). In all experiments, a single-part heat-cured highly-toughened epoxy adhesive was used.

2.2. Fatigue testing

All fatigue experiments were carried out at a cyclic frequency of 20 Hz in a desiccant chamber to achieve a dry condition (11–15% relative humidity). The experiments were conducted under displacement control, with a constant displacement ratio, $R = \delta_{min}/\delta_{max} = 0.1$, measured at the loading pins. The tests began with application of the highest strain energy release rate, G , which then decreased as the crack grew under constant loading pin displacement until the threshold crack growth rate (10^{-6} mm/cycle) was reached at the threshold strain energy release rate, G_{th} . It was previously shown that testing under force or displacement control does not significantly affect the fatigue behavior [20].

The unloading joint compliance approach [23] was used to measure the fatigue crack length. The joint compliance was measured during the unloading portion of the cycle using the load cell output and a clip gauge attached to the end of the specimen. A CCD camera (2 mm field of view) on a motorized linear stage was used to measure the crack length and relate it to the measured joint compliance for a given specimen type, using the approach of Ref. [24]. A least squares regression was used to fit a third-order polynomial, with c_1 to c_4 as the constants, to the normalized crack length, a/w , versus the normalized specimen compliance, CEB , for fatigue joints:

$$a/w = c_1 \times (CEB)^3 + c_2 \times (CEB)^2 + c_3 \times (CEB) + c_4 \quad (1)$$

where a is the crack length, w is the specimen length from the loading pins, C is the compliance, E is the tensile modulus of the adherends, and B is the specimen width. Eq. (1) produced a good fit to the experimental data ($R^2 = 0.997 \pm 0.2$).

2.3. Fracture testing

The fracture tests were performed on aluminum ADCB joints. The same load was applied on the both arms of the ADCB at a constant cross-head speed of 1 mm/min to produce a mixed-mode loading condition ($\psi = 18^\circ$) at the crack tip. The crack length was measured from the center of the loading pins to the tip of the macro-crack on the ADCB specimens using a microscope mounted on a micrometer stage. Crack growth was stable in this system so that many crack extension events could be recorded with a single ADCB specimen. To measure the critical load at each crack length, the cross-head displacement was started and stopped repeatedly in the vicinity of the expected fracture load (each time at a constant cross-head speed of 1 mm/min) until a drop in the applied load was observed. This maximum load prior to the drop was taken as the critical fracture load for the measured crack length if visual inspection through the microscope confirmed that the macro-crack had propagated. After measuring the new macro-crack length, the ADCB was unloaded and the same procedure was followed again beginning at the new crack length. For the present adhesive system, it was previously shown that defining the crack length based on the macro-crack rather than the furthest advanced micro-crack had a very small effect on the measured G_c [25]. As well, it is noted that such micro-cracking is only observable in fracture tests and at relatively high fatigue crack growth rates, where the applied strain energy release rates are much higher than those used in the fatigue threshold region.

It was also of interest to measure the effect of bondline thickness on the mode-I and mixed-mode critical strain energy release rate for fracture from an existing fatigue crack corresponding to the fatigue threshold where the plastic zone and process zone were very small. This value was denoted G_{c0} , and was defined as the first crack extension of approximately 50 μm from the fatigue precrack corresponding to G_{th} .

2.4. Strain energy release rate calculation

The strain energy release rate, G , for DCB and ADCB joint was calculated from the measured force and crack length using an analytical beam-on-elastic-foundation model [21]. These predicted G values for aluminum and steel DCB and ADCB joints were within 2% of those predicted from a two-dimensional elasto-plastic finite element model for crack lengths of 40–120 mm, typical crack lengths in the conducted experiments [21]. The elastic moduli of the adherend and the adhesive were 68.9 GPa and 1.5 GPa, respectively. The adhesive's stress-strain curve [19] was obtained experimentally from tensile tests, performed by the adhesive manufacturer.

3. Experimental results and discussion

3.1. Fatigue tests

Fig. 2 shows that increasing the bondline thickness from 130 μm to 380 μm doubled G_{th} under mode-I loading. However, no further statistically significant improvement in G_{th} was observed by increasing the adhesive thickness to 790 μm (t -test, 95% confidence). The threshold under mixed-mode loading depended only slightly on the bondline thickness in the studied range; the only statistically significant difference was between G_{th} at the largest (790 μm) and smallest (130 μm) bondline

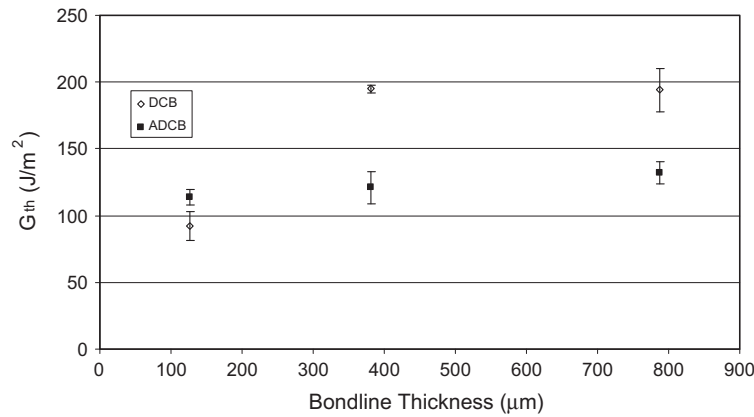


Fig. 2. Effect of bondline thickness on G_{th} of DCB specimens (mode-I) and ADCB specimens (mixed-mode). Six threshold measurements were performed for ADCBs at $t = 380 \mu\text{m}$, with three measurements at the other conditions. Error bars represent ± 1 standard deviation.

thickness (t -test, 95% confidence). Under mode-I loading, the fatigue failure was cohesive in the mid-plane of the adhesive for all the tested bondlines and crack growth rates. The mixed-mode fatigue failure was also fully cohesive in the adhesive, except for some patches of interfacial failure, covering up to about 1/3 of the fracture surface at the threshold of the 130 μm ADCB joints.

Figs. 3 and 4 show the measured fatigue crack growth rates versus G_{max} , the maximum energy release rate in a cycle, for all the tested DCB and ADCB specimens. For the sake of clarity, only three of the six experiments are shown for the mixed-mode ADCB joints with $t = 380 \mu\text{m}$. The fatigue results were very repeatable for both the DCB and ADCB joints, showing two distinct regions, a linear region (Paris law region) at higher crack growth rates, and a threshold region. To show the effect of bondline thickness on the crack growth rate behavior, a least squares regression line (Eq. (2)) was fitted to all the data in the linear region at each mode ratio and bondline thickness,

$$\log(da/dN) = m \times \log(G_{max}) + b \quad (2)$$

where a and N are the crack length and the cycle number, respectively, with m and b being the constants calculated from the regression fit.

Fig. 5a shows that the crack growth rates for $t = 380 \mu\text{m}$ and $790 \mu\text{m}$ were very similar when the crack was close to the threshold region under mode-I loading, but there was a small decrease in crack growth rate with increasing bondline thickness as G_{max} increased. The crack growth rate at $t = 130 \mu\text{m}$ was significantly higher than at $t = 380$ and $790 \mu\text{m}$ (t -test, 95% confidence). Overall, as the crack speed increased, the effect of bondline thickness on the fatigue performance became more pronounced (Fig. 5a).

For mixed-mode loading, Fig. 5b, the crack growth rates were similar for the three bondline thicknesses when the crack speed was in the threshold region. As G_{max} increased, however, the crack growth rate for the thinnest adhesive layer, $t = 130 \mu\text{m}$, increased significantly. The crack growth rates for $t = 380 \mu\text{m}$ and $790 \mu\text{m}$ were indistinguishable (t -test, 95% confidence). As with the DCB joints, the effect of bondline thickness on the fatigue performance became more pronounced as the crack growth rate (or G_{max}) increased. For example, at $G = 400, 800$ and 1200 J/m^2 , the fatigue crack in the thinnest joint ($t = 130 \mu\text{m}$) propagated 3, 8 and 11 times faster than that in the thicker joint ($t = 380 \mu\text{m}$).

The effect of bondline thickness on fatigue and fracture performance is usually explained in terms of the effect of adherend constraint on the damage zone or plastic zone in the adhesive layer. It is recognized that the fracture process zone encompasses several damage mechanisms (e.g. void creation, micro-cracking, stretching of rubber particles, plasticity); therefore, the plastic zone is a surrogate for the actual damage zone, and it is assumed that trends concerning the effect of constraint on the plastic zone will also be evident in reality where a damage zone exists in and around the plastic zone. The plastic zone is usually defined as the region in which the von Mises stress is greater than or equal to the yield stress or proportional limit of the adhesive [6,19]. As the plastic zone becomes smaller, the effect of the substrate on the plastic zone shape and size is reduced, and at some point, the plastic zone becomes too small to be affected by the adherend constraint. The plastic zone size depends on the applied load and the mechanical properties of the adhesive and adherends. As the applied force, and thus the applied G decreases, the plastic zone becomes smaller. This may explain the experimentally observed trend that the effect of bondline thickness becomes less pronounced at lower crack growth rates, when the applied G_{max} is also lower. However, since the bond toughness is equal to the sum of the energy dissipation in the fracture process zone, Γ_0 (due to void nucleation and bond breakage) and the plastic dissipation in the adhesive layer, Γ_p , [26], considering only the plastic zone ignores any possible effect of adhesive thickness on Γ_0 . The effect of adherend constraint on the stress distribution and the plastic zone ahead of the crack tip in the adhesive layer under both mode-I and mixed-mode loading will be considered in detail using finite element modeling in the accompanying paper [19].

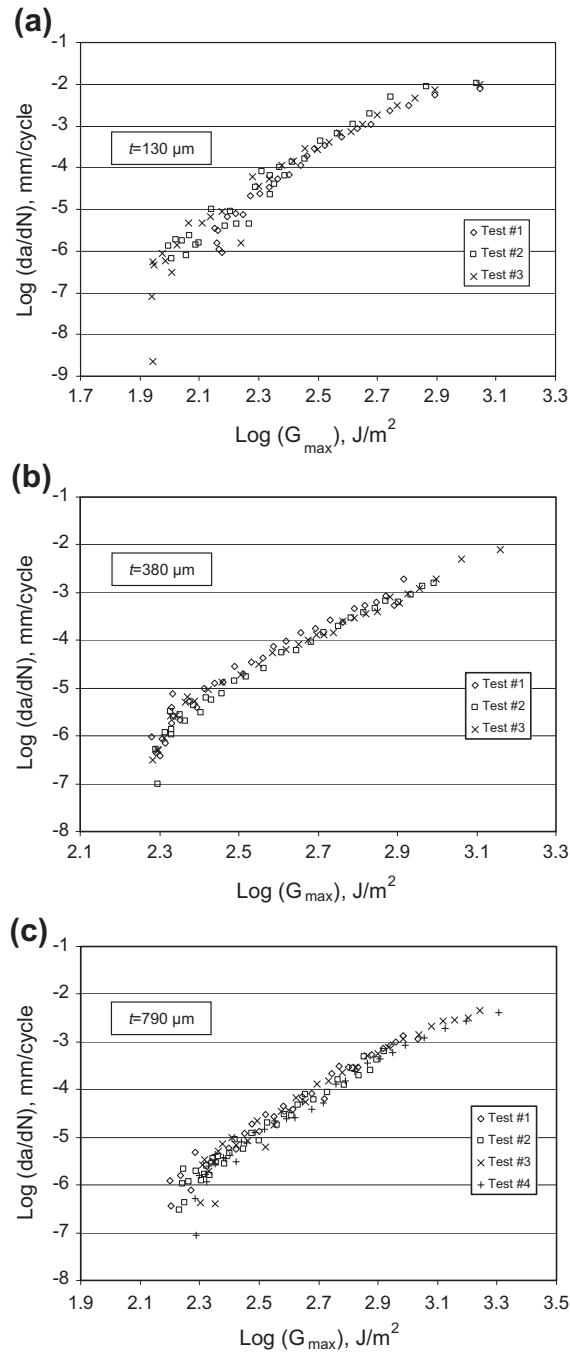


Fig. 3. Fatigue crack growth rates for mode-I DCB specimens with bondline thicknesses of (a) 130 μm , (b) 380 μm and (c) 790 μm .

As shown in Figs. 2 and 5b, the mixed-mode G_{th} did not change appreciably with bondline thickness. Since the majority of practical joints are loaded under mixed-mode conditions, the relatively low sensitivity of the mixed-mode G_{th} to the bondline thickness has important implications for adhesive joint design based on the fatigue threshold. For instance, in many industrial applications, accurate control over the adhesive thickness is not feasible; however, the present results indicate that such control may not be necessary under mixed-mode loading conditions. Furthermore, the measurement of G_{th} at a single bondline thickness for the desired range of phase angles is probably sufficient in most cases.

Fatigue cycling may increase the crack tip temperature due to viscous dissipation, although the effect is usually relatively small. For example, the maximum crack tip temperature increased by less than 1 $^{\circ}\text{C}$ in rubber-toughened epoxies tested at 1–100 Hz [27], and approximately 10 $^{\circ}\text{C}$ in nylon and polyester composites tested at 20 Hz in the Paris law crack growth

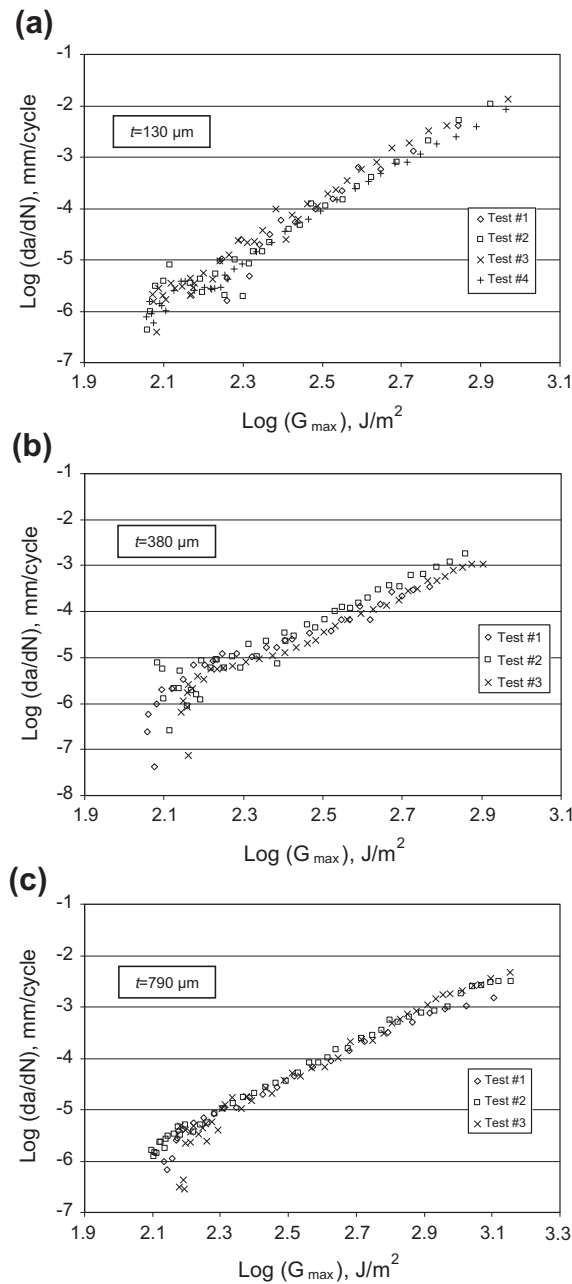


Fig. 4. Fatigue crack growth rates for mixed-mode ADCB specimens with bondline thicknesses of (a) 130 μm , (b) 380 μm and (c) 790 μm .

regime [28]. The increase in temperature in aluminum adhesive joints would be much smaller due to the rapid heat dissipation provided by the adherends. Moreover, Datla et al. [29] showed that for the present adhesive system, the fatigue threshold was virtually independent of the testing temperature from 20 °C to 80 °C. Therefore, any effects of a small increase in adhesive temperature due to viscous damping were ignored.

3.2. Fracture tests

Quasi-static fracture tests using ADCB specimens produced a typical R -curve behavior [30]. After onset of fracture at G_{c0} , the first several crack growth sequences occurred at an increasing critical energy release rate, G_c , as the damage zone at the crack tip developed to its steady-state form [31] (Fig. 6). The steady-state critical strain energy release rate, G_c^s , was considered to be the average value over this “plateau” (steady-state) region. The crack path was cohesive (within the adhesive) in all cases.

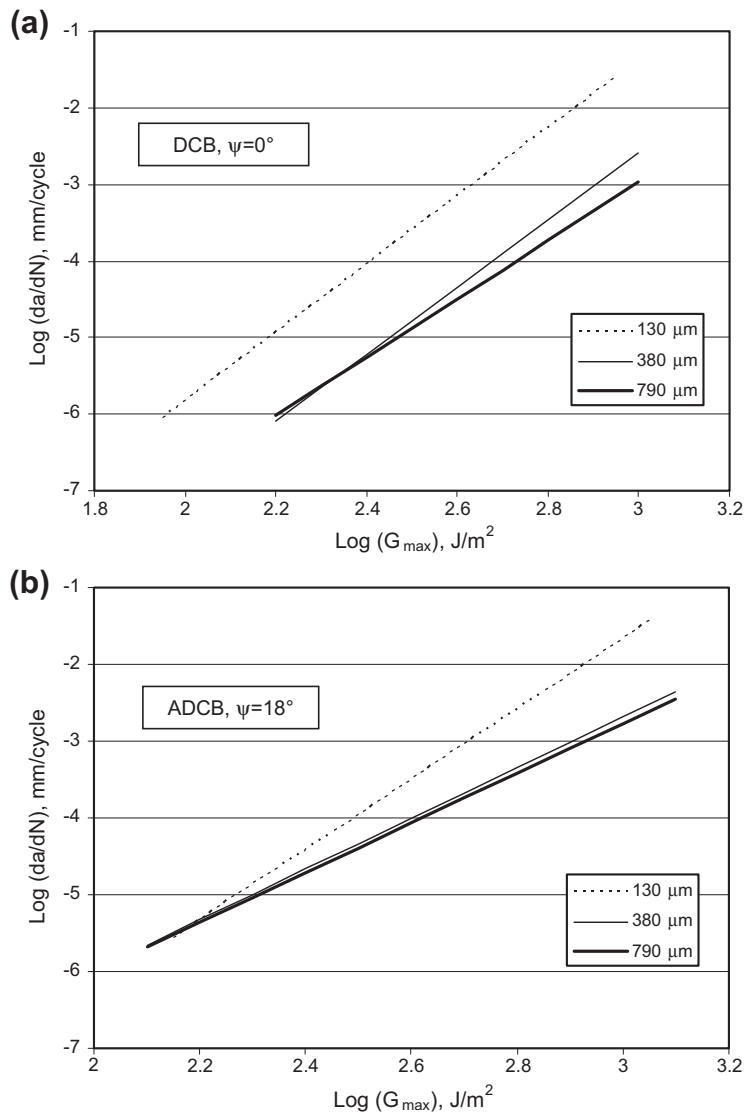


Fig. 5. Effect of bondline thickness on fatigue crack growth rate at different strain energy release rates for (a) mode-I loading and (b) mixed-mode loading. The lines are the best fits to the Paris law (linear) region in each of Figs. 3 and 4.

The effect of bondline thickness on G_{c0} measured from the fatigue threshold precrack is shown in Figs. 7 and 8 for DCB and ADCB joints, respectively. G_{c0} increased with bondline thickness under mode-I loading (Fig. 7), but the decreasing slope suggested an approach to a plateau. A similar trend was observed under mixed-mode loading (Fig. 8), although a plateau value of G_{c0} may already have been reached since the values at 380 μm and 790 μm were indistinguishable (*t*-test, 95% confidence). As is typical of crack initiation measurements, there was a relatively large scatter in the experimental results due to microscopic differences in the local geometry and adhesive composition and uncertainties in the detection of crack initiation [32]. The latter is compounded by the inability to observe initiation at locations other than the single side viewed by the microscope.

Comparing Figs. 7 and 2 show that both G_{c0} and G_{th} exhibited a somewhat similar trend with bondline thickness under mode-I loading. The same can be said under mixed-mode conditions (Figs. 8 and 2). These observations are not too surprising since fatigue crack propagation near the threshold and the onset of fracture both involve minute amounts of crack extension from a relatively small damage zone (low G). They do indicate that strain rate effects were small with this adhesive over this range of loading conditions, since the fatigue tests were conducted at 20 Hz while the fracture initiation was quasi-static.

Bondline thickness had a large effect on the quasi-static critical strain energy release rate, G_c^s , as shown in Fig. 9. The standard deviations were based on 24, 87 and 46 data points on the plateaus of the *R*-curves at $t = 130 \mu\text{m}$, 380 μm and 790 μm , respectively. Three specimens were tested at $t = 380 \mu\text{m}$, and one at each of the other two thicknesses. Previous experience

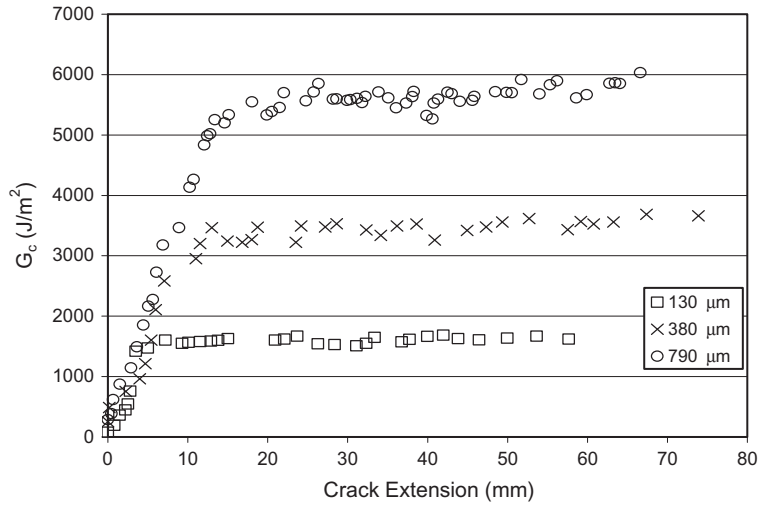


Fig. 6. R-Curve behavior of ADCB joints at different bondline thicknesses.

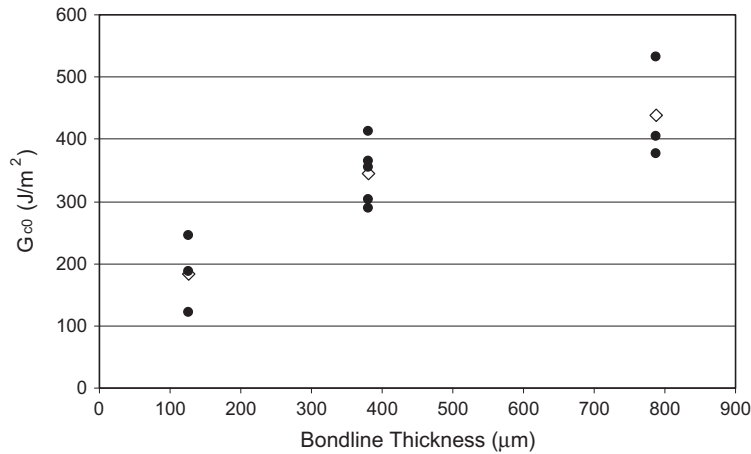


Fig. 7. Effect of bondline thickness on the average mode-I quasi-static strain energy release rate for the onset of fracture from the fatigue threshold, G_{c0} . Five measurements were performed at $t = 380 \mu\text{m}$, with three measurements at the other two bondline thicknesses. Black dots show each G_{c0} measurement, with the average at each adhesive thickness given with the hollow diamond.

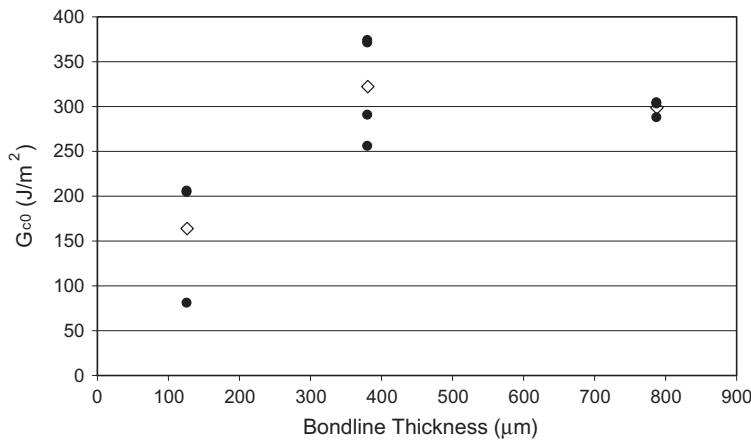


Fig. 8. Effect of bondline thickness on the average mixed-mode quasi-static strain energy release rate for the onset of fracture from the fatigue threshold, G_{c0} . Four measurements were performed at $t = 380 \mu\text{m}$, and three measurements at the other two bondline thicknesses. Black dots show each G_{c0} measurement, with the average at each adhesive thickness given with the hollow diamond.

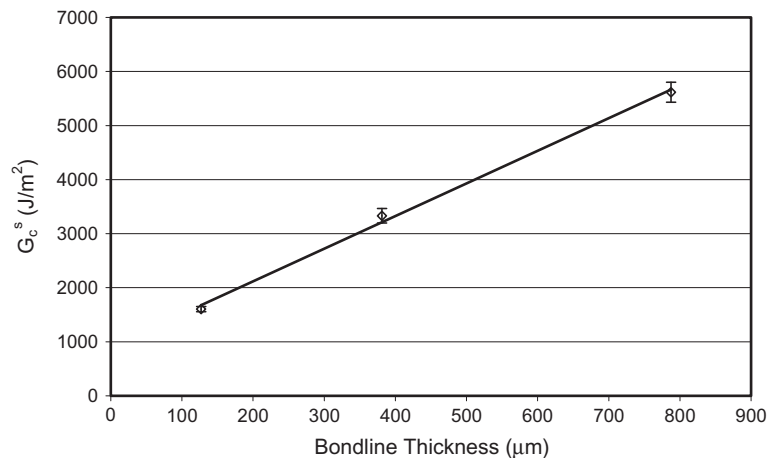


Fig. 9. Effect of bondline thickness on the mixed-mode (18°) quasi-static steady-state critical strain energy release rate, G_c^s . Error bars represent ± 1 standard deviation. The black line is the least-squares fit.

with fracture testing of this adhesive showed a very good repeatability [25]. The strong dependence of G_c^s on bondline thickness was due to the large plastic zone size at the tip of the fully developed crack in this highly-toughened epoxy adhesive. This is discussed further in Part II [19]. It is expected that the trend of Fig. 9 would be followed by a maximum at some optimum bondline thickness, as has been observed for other toughened epoxies [4–6,14] and was predicted by the finite element analysis of Part II [19]. However, this was not explored since adhesive thicknesses above 800 μm are not of practical interest in most applications.

It is expected that the data of Fig. 9 would also apply to mode-I fracture, since G_c^s is only very weakly dependent on phase angle ψ , when $\psi < 30^\circ$, as was demonstrated for the present adhesive system in [25].

4. Conclusions

The effect of bondline thickness on fatigue behavior became more pronounced as the applied G and the crack growth rate increased. The crack growth rate was more sensitive than the fatigue threshold to changes in the adhesive thickness.

Under mixed-mode loading, a very small effect of bondline thickness on the mixed-mode fatigue threshold was observed. This observation may simplify the design of adhesive joints for fatigue loading.

The critical strain energy release rate for quasi-static fracture increased linearly with bondline thickness from 130–780 μm .

Acknowledgements

The authors acknowledge the Natural Sciences and Engineering Research Council of Canada, the Ontario Centres of Excellence, and General Motors of Canada for their financial support.

References

- [1] Mall S, Ramamurthy G. Effect of bond thickness on fracture and fatigue strength of adhesively bonded composite joints. *Int J Adhes Adhes* 1989;9:33–7.
- [2] Abou-Hamda MM, Megahed MM, Hammouda MMI. Fatigue crack growth in double cantilever beam specimen with an adhesive layer. *Engng Fract Mech* 1998;60:605–14.
- [3] Chai H. Fracture work of thin bondline adhesive joints. *J Mater Sci Lett* 1988;7:399–401.
- [4] Chai H. Bond thickness effect in adhesive joints and its significance for mode I interlaminar fracture of composites. In: *Composite materials testing and design*. ASTM-STP 893; 1986. p. 209–31.
- [5] Bascom WD, Cottingham RL, Jones RL, Peyser P. The fracture of epoxy and elastomer-modified epoxy polymers in bulk and as adhesives. *J Appl Polym Sci* 1975;19:2545–62.
- [6] Kinloch AJ, Shaw SJ. The fracture resistance of a toughened epoxy adhesive. *J Adhes* 1981;12:59–77.
- [7] Hunston DL, Kinloch AJ, Wang SS. Micromechanics of fracture in structural adhesive bonds. *J Adhes* 1989;28:103–14.
- [8] Daghiyani HR, Ye L, Mai Y-W. Mode-I fracture behaviour of adhesive joints part I. relationship between fracture energy and bond thickness. *J Adhes* 1995;53:149–62.
- [9] Schmueser DW, Johnson NL. Effect of bondline thickness on mixed-mode debonding of adhesive joints to electroprimed steel surfaces. *J Adhes* 1990;32:171–91.
- [10] Kahramana R, Sunarb M, Yilbas B. Influence of adhesive thickness and filler content on the mechanical performance of aluminum single-lap joints bonded with aluminum powder filled epoxy adhesive. *J Mater Process Technol* 2008;205:183–9.
- [11] daSilva LFM, Carbas RJC, Critchlow GW, Figueiredo MAV, Brown K. Effect of material surface treatment and environment on the shear strength of single lap joints. *Int J Adhes Adhes* 2009;29:621–32.

- [12] Madhusudhana KS, Narasimhan R. Experimental and numerical investigations of mixed mode crack growth resistance of a ductile adhesive joint. *Engng Fract Mech* 2002;69:865–83.
- [13] Kawashita LF, Kinloch AJ, Moore DR, Williams JG. The influence of bond line thickness and peel arm thickness on adhesive fracture toughness of rubber toughened epoxy–aluminium alloy laminates. *Int J Adhes Adhes* 2008;28:199–210.
- [14] Pardoën T, Ferracin T, Landis CM, Delannay F. Constraint effects in adhesive joint fracture. *J Mech Phys Solids* 2005;53:1951–83.
- [15] Taib AA, Boukhili R, Achiou S, Gordon S, Boukehili H. Bonded joints with composite adherends. Part I. Effect of specimen configuration, adhesive thickness, spew fillet and adherend stiffness on fracture. *Int J Adhes Adhes* 2006;26:226–36.
- [16] Joseph R, Bell JP, McEviley AJ, Liang JL. Fatigue crack growth in epoxy/aluminum and epoxy/steel joints. *J Adhes* 1993;41:169–87.
- [17] Xu XX, Crocombe AD, Smith PA. Fatigue crack growth rates in adhesive joints tested at different frequencies. *J Adhes* 1996;58:205–26.
- [18] Schmueser DW. A fracture mechanics approach to characterizing cyclic debonding of varied thickness adhesive joints to electroprimed steel surfaces. *J Adhes* 1991;36:1–23.
- [19] Azari S, Papini M, Spelt JK. Effect of adhesive thickness on fatigue and fracture of toughened epoxy joints – part II. Analysis and finite element modeling. *Engng Fract Mech* 2011;78:138–52.
- [20] Azari S, Papini M, Schroeder JA, Spelt JK. Fatigue threshold behavior of adhesive joints. *Int J Adhes Adhes* 2010;30:145–59.
- [21] Azari S, Papini M, Schroeder JA, Spelt JK. The effect of mode ratio and bond interface on the fatigue behavior of a highly-toughened epoxy. *Engng Fract Mech* 2010;77:395–414.
- [22] Wegman RF. Surface preparation techniques for adhesive bonding. New Jersey: Noyes Publications; 1989.
- [23] Davies P. Protocols for interlaminar fracture testing of composites. Polymer and Composites Task Group, European Structural Integrity Society; 1992.
- [24] Standard test method for measurement of fatigue crack growth rates, ASTM E647. American society for testing and materials; 2000.
- [25] Azari S, Eskandarian M, Papini M, Schroeder JA, Spelt JK. Fracture load predictions and measurements for highly toughened epoxy adhesive joints. *Engng Fract Mech* 2009;76:2039–55.
- [26] Martiny P, Lani F, Kinloch AJ, Pardoën T. Numerical analysis of the energy contributions in peel test: a steady-state multilevel finite element approach. *Int J Adhes Adhes* 2008;28:222–36.
- [27] Hwang J-F, Manson JA, Hertzberg RW, Miller GA, Sperling LH. Fatigue crack propagation of rubber-toughened epoxies. *Polym Engng Sci* 1989;29:1477–87.
- [28] Lang RW, Manson JA. Crack tip heating in short-fibre composites under fatigue loading conditions. *J Mater Sci* 1987;22:3576–80.
- [29] Datla NV, Papini M, Spelt JK. Effect of humidity and temperature on the fatigue behavior of a toughened epoxy adhesive. In: Proceedings of 33rd annual meeting of adhesion society, Daytona Beach, FL; 2010. p. 41–3.
- [30] Hutchinson JW, Suo Z. Mixed mode cracking in layered materials. In: Hutchinson JW, Wu TY, editors. *Advances in applied mechanics*, vol. 29. New York: Academic Press Inc.; 1992. p. 63–191.
- [31] Papini M, Fernlund G, Spelt JK. The effect of geometry on the fracture of adhesive joints. *Int J Adhes Adhes* 1994;14:5–13.
- [32] Ameli A, Papini M, Schroeder JA, Spelt JK. Fracture R-curve characterization of toughened epoxy adhesives. *Engng Fract Mech* 2010;77:521–34.